Semnan University

Journal of Heat and Mass Transfer Research

Journal homepage: https://jhmtr.semnan.ac.ir

ISSN: 2383-3068

Research Article

Numerical Study of Temperature Field of Tinplate in the Quench Process

Ali Jafari, Ahmad Reza Rahmati *

Department of Mechanical Engineering, University of Kashan, Kashan, Iran

ARTICLE INFO

Article history:

Received: 2024-10-12
Revised: 2025-05-24
Accepted: 2025-06-10

Keywords:

Quench process;
Tinplate;
Temperature field;
Modeling;
Volume of fluid.

ABSTRACT

The tinplate quenching process at Mobarakeh Steel Company was analyzed for the first time using computational fluid dynamics to reduce the defect in the quench spot on the tinplate's surface. The volume of a fluid model was used to simulate the process. The effect of nozzle angle equal to 15, 30, and 45 degrees, nozzle jet velocities of about 10 and 8 m/s, tinplated velocities of 244, 200, and 160 m/min, and cooling fluid temperature of 30, 40, and 55 °C on the tinplate temperature field was investigated. Results show that the tinplate temperature field is relatively uniform at a 45° nozzle angle. In addition, a more uniform temperature field was obtained by increasing the nozzle jet velocity from 8 m/s to 10 m/s and decreasing the tinplate velocity from 244 m/min down to 160 m/min.

1. Introduction

Tinplates are steel sheets with a thin layer of tin to prevent corrosion and rust as well as increase brightness [1]. In the field of tinplate application, which is mostly related to the packaging industry, surface quality is a critical index, which greatly impacts its corrosion rate [2]. The processes involved in the production of tinplates such as hot rolling, cold rolling, annealing, and secondary cold rolling can lead to the creation of some quality defects on the substrate's surface of the tinplate such as the oxidation sheet, slag inclusion, and emulsion stain [3, 4], whereas, the plating process of steel plate with tin layer mainly produces quality defects such as quench stain, pinholes, and wavy surfaces on the surface of tinplate [5, 6].

Tinplate production generally includes washing the steel plate, initial tin coating, heat treatment to melt the tin coating, rapid cooling of the plate-molten tin and finally creating a layer of chrome coating to prevent further oxidation. The heat treatment is performed around the melting point of tin around 232°C to 265°C. The next step is rapid cooling of the coated plate through the quench process by passing the hot plate through a quench tank containing a submerged jet impingement [7]. Combining the heat treatment with the quenching process stabilizes the tin layer on the sheet surface which strongly improves the surface quality and properties of this product [8]. Distortion of the plate and cracking of the tin layer can occur due to inhomogeneous cooling and undesired heat transfer during the quenching process, which

* **Corresponding author.**
E-mail address: *ar_rahmati@kashanu.ac.ir*

Cite this article as:

Jafari, A. and Rahmati, A. R., 2026. Numerical Study of Temperature Field of Tinplate in the Quench Process. *Journal of Heat and Mass Transfer Research*, 13(1), pp. 137-146.

https://doi.org/10.22075/JHMTR.2025.35119.1618

affects the quality of the produced parts [9]. Fixing defects caused by the tin coating increases the quality of these tinplates. Non-uniform fluid flow in the quench tank is another cause of quench defects, tin coating cracking, and distortion. Therefore, a uniform temperature field and hemogenic distribution of fluid flow in the quench zone are critical to prevent quench defects [10]. This process can be controlled by operating conditions and influencing parameters. In this regard, various parameters affect the cooling rate and change of the temperature field on the tinplate. These parameters include the plate passing speed, nozzle configuration, nozzle jet speed, nozzle pressure, nozzle angle, and water temperature [11, 12]. Therefore, investigating the effect of each variable on controlling the conditions and improving the quality of the tinplate quality, such as reducing quality defects, removing the quench spot, and removing the edge wave defect is important. The quenching process of tinplates presents great complexity due to the high speed of the plates' passage and the short time scale of passing that characterizes the field temperature [12]. Gomes et al. [12] investigated the effects of plate speed and water temperature on the quenching process and reported that increasing the plate speed seriously prevents heat transfer. Although many experimental studies have been reported on the quenching process of steel plates that pass through the quench tank at high speed, research on the field temperature and cooling rate of this process remains a global challenge due to the moving state of the plate and complex boiling regimes [12-14].

The design and optimization of various systems requires conducting various experiments and tests, which are usually very expensive and time-consuming, and the design and construction process faces many challenges [15]. With the progress and development of computing software, it is possible to investigate many complex processes. It is possible to find conditions affecting the control and efficiency of the process through simulation [16]. In this context, the computational fluid dynamics (CFD) method is considered one of the most powerful numerical methods for simulating and evaluating the quenching process [17, 18]. Kobayashi et al. [19] developed a computational fluid dynamics simulation model for the quenching process of a hot steel plate with the help of impinging water jets with a cylindrical cross-section. Toghraie et al. [20] presented a numerical method for simulating the quenching of a hot surface at a temperature of 800 °C using the volume of fluid method. They reported that the convective heat transfer coefficient at the stagnation point increased with the increase in the water fluid jet speed. Qu et al. [21] designed a physical model of strong quench equipment with a double vortex flow field and used Fluent software to investigate and optimize the quench tank flow field. Gadala et al. [22] presented a numerical study of two-phase cooling during the quenching process of a steel plate using computational fluid dynamics and the volume of fluid method for impinging a water jet with a circular cross-section on a hot steel plate. However, the temperature field of the quenching process of the tinplates and the evaluation of the variables effective in reducing the quenching defects using computing software have not been well studied.

This research aims to investigate the effect of nozzle angle, water jet velocity, tinplate velocity, and cooling water temperature on the cooling rate and temperature field in the quenching process in Isfahan's Mobarakeh Steel Company, which is one of Iran's largest tinplate producers in Iran. This study was conducted for the first time to optimize and evaluate quenching conditions for Mobarakeh Steel Company based on computational methods. CFD simulation using fluid volume was used for the simulation.

2. Methodology

This study simulates the quenching process used in Mobarakeh Steel Company's tinplate unit. For this purpose, the process geometry, including the quenching tank, tinplate, and nozzles, was designed using SolidWorks software. Mesh was applied to the solids and fluids domain. Finally, the simulation was performed using Fluent software based on the determined geometry and conditions. This study used the volume of the fluid model to simulate the quenching process.

2.1. Governing Equations

The quench severity is relevant to the heat exchange rate between hot tinplate and cold media which depends on various parameters such as cooling water condition, water-jet velocity, and the exposure time of the tinplate to cooling water. Navier-Stokes equations contain conservation equations for Momentum, Mass, and Energy, according to Eq. 1 - Eq. 3, can be applied as a theoretical approach to describing this heat exchange relationship. The continuity assumption and incompressibility fluid have been applied in these equations [23].

Here, the fluid model volume has been used to model the quenching process. The following simplified assumptions are considered in the current study for the flow field, quenching tank, and tinplate:

(i). The water cooling fluid was considered incompressible.

(ii). The phase change enthalpy of molten tin from molten state to solid state was assumed negligible.

(iii). The flow was considered as a turbulent flow.

(iv). Due to the low thickness of the plate, the heat transfer in the tinplate thickness direction is negligible.

$$\frac{\partial(\alpha_l\rho_l)}{\partial t} + \vec{\nabla}.\left(\alpha_l\rho_l\vec{v}_l\right) = \dot{m}_{lv} \tag{1}$$

$$\frac{\partial\left(\alpha_l\rho_l\vec{v}_l\right)}{\partial t} + \vec{\nabla}.\left(\alpha_l\rho_l\vec{v}_l\vec{v}_l\right) = -\alpha_l\vec{\nabla}p + \vec{\nabla}.\bar{\bar{\tau}}_l + \alpha_l\rho_l\vec{g}_l + \dot{m}_{lg}\vec{v}_{lg} + \vec{F}_{lg} \tag{2}$$

$$\frac{\partial\left(\alpha_l\rho_l h_l\right)}{\partial t} + \vec{\nabla}.\left(\alpha_l\rho_l\vec{v}_l h_l\right) = -\alpha_l\frac{\partial p}{\partial t} + \bar{\bar{\tau}}_l:\vec{\nabla}\vec{v}_l + \dot{m}_{lg}h_{lg} + Q_{lg} \tag{3}$$

here, l represents the water fluid phase and g is water vapor fluid phase. ρ and $\vec{v}$ represent the density and velocity vectors, respectively. $\dot{m}_{lg}$ shows the volumetric mass exchange rate between phases l and g. In the volume of fluid method, the α phase indicator shows the volume ratio in the form of the volume of one phase to the cell volume. In these equations, αl is equal to 1 in the liquid phase, zero in the vapor phase, and has a value between zero and 1 in the liquid-vapor interface region. The term $\bar{\bar{\tau}}_l$ is the molecular stress tensor applied to phase l, and the term F_{lg} represents the interfacial momentum transfer caused by drag and non-drag forces. p indicates the pressure forces and $\vec{g}$ shows the gravitational acceleration vector. In Eq. 3, h represents enthalpy, $\vec{q}$ is the heat flux vector, Q_{lg} is the energy exchange between the two phases and h_{lg} is the enthalpy difference between the two phases [24].

The turbulent flow model is considered realizable k-ε model. This model is a subset of K-Epsilon turbulence models, which provide good results for problems with free flow including fluid jets, flow including rotation, separation and high strain rates. This model differs from the standard k-ε model and includes a new form of perturbed viscosity. The modeled transmission equations for k and ε in the realizable k-ε model are Eq. 4, and Eq. 5 [24].

$$\frac{\partial}{\partial t}(\rho k) + \frac{\partial}{\partial x_j}(\rho k u_j) = \frac{\partial}{\partial x_j}\left[(\mu + \frac{\mu_t}{\partial_k})\frac{\partial K}{\partial x_j}\right] + P_k + P_b - \rho\epsilon - Y_m + S_k \tag{4}$$

$$\frac{\partial}{\partial t}(\rho\epsilon) + \frac{\partial}{\partial x_j}(\rho\epsilon u_j) = \frac{\partial}{\partial x_j}\left[\left(\mu + \frac{\mu_t}{\sigma_\epsilon}\right)\frac{\partial\epsilon}{\partial x_j}\right] + \rho C_1 S_\epsilon - \rho C_2\frac{\epsilon^2}{k + \sqrt{v\epsilon}} + C_{1\epsilon}\frac{\epsilon}{k}C_{3\epsilon}P_b + S_\epsilon \tag{5}$$

in these equations, P_k represents turbulence kinetic energy generation due to mean velocity gradients and P_b represents turbulence kinetic energy generation due to buoyancy. Also, Y_M is the contribution of fluctuating expansion in compressible turbulence to the overall loss rate. C_2, and $C_{1\epsilon}$ constants are equal to 1.9, and 1.44, respectively. The values of σk and σϵ are equal to 1 and 1.2, respectively. Here, C_1, is according to the relations presented in Eq. 6. Also, η, and S are in accordance with Eq. 7, and Eq. 8.

$$C_1 = max\left[0.43 + \frac{\eta}{\eta + 5}\right] \tag{6}$$

$$\eta = S\frac{k}{\epsilon} \tag{7}$$

$$S = \sqrt{2S_{ij}S_{ij}} \tag{8}$$

2.2. Geometry Modelling

The schematic geometry of the under-study tinplate, quench tank, and water nozzles is shown in Figure 1. Briefly, this process consists of a hot steel sheet (width 700 mm and thickness 0.3 mm) at a temperature of 505 K, coated with a thin layer of molten tin (thickness of 2.8 g/m^2) on both sides of the plate, which passes through the tank at a velocity of 244 m/min. After cooling, it exits the tank from the other side on a roller. The temperature of the cooling water in the quenching tank is 303 K which is adjustable between 303 and 328 K. The water level in the quenching tank is constant. In this tank, 30 cm below the water level, there are a series of water nozzles with a circular cross-section of 5 mm diameter on both sides of the plate, which inject water at a velocity of 8 m/s to the surface of the plate. An infinite length was assumed for this tinplate. Table 1 lists the geometric parameters of the quenching tank, tinplate, and initial conditions.

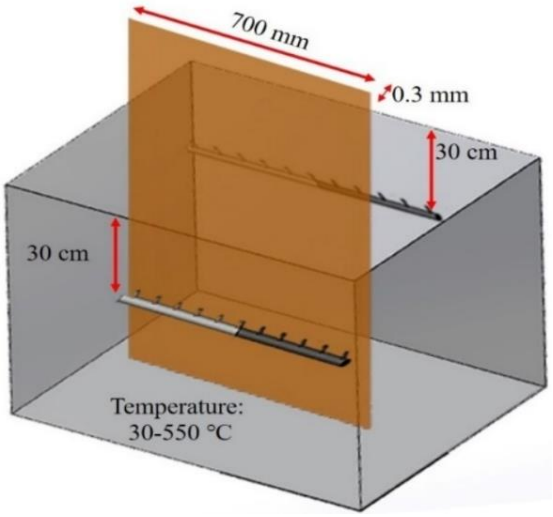

Fig. 1. Schematic geometry of the under-study tinplate, quench tank, and water nozzles

First, the geometry of the fluid domain of the quenching tank, tinplate, and nozzles was designed in SolidWorks software. Figure 2 shows a view of the geometry designed in SolidWorks software. The fluid domain includes water-spraying nozzles on both sides of the plate.

Table 1. Parameters of quench tank, plate, and initial conditions

Geometric Parameter	Unit	Values
Nozzle Angle	degree	15, 30, 45
Water jet Velocity	m/s	8, 10
Tinplate Value	m/min	244, 200, 160
Water Temperature	K	303, 313, 328

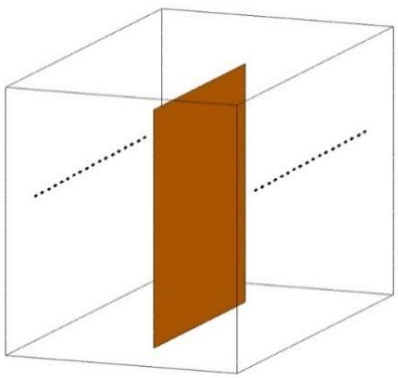

Fig. 2. View of the designed geometry

2.3. *Meshing*

The meshing design was performed with Ansys meshing software. The solver was selected as Fluent, and the element size was set to 20 mm. The option of "capture curvature" was activated to increase the meshing quality and accuracy, and the minimum size of the elements was set to 0.2 mm with a growth factor of 1.2. This operator increases the mesh density in curved or pointed parts. After applying these settings, about 881479 elements were created as disordered elements in the flow field. Figure 3 shows a view of the meshing results of the flow field in the quenching tank and meshing results in the tinplate. As can be seen, the meshing density near the nozzles and near the tinplate edges is higher than in other parts.

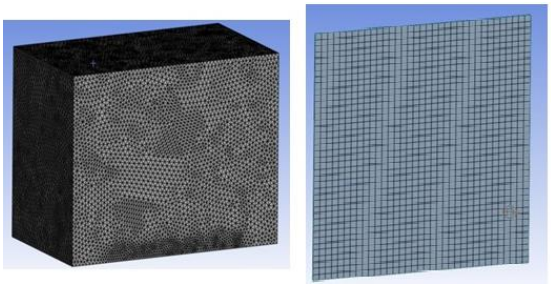

Fig. 3. View of the designed meshing in (a) flow field in quenching tank; (b) tinplate

2.4. Boundary Conditions and Parameters Setting

After importing the designed geometric model into the Ansys Fluent software, the parameters and conditions for simulation were set, according to Table 2. Gravity was selected in the downward -y direction in the gravity section. Also, due to the incompressibility of water and the rapid passage of the tinplate, the cooling process was defined as unsteady and the transient option was selected in the time section. The water jet velocity from the nozzles was considered a velocity inlet type. The upper part of the quenching tank is of a pressure outlet type, which means atmospheric pressure at that boundary. The surfaces of the quenching tank were considered wall type with the condition of non-slip.

Table 2. Details of the parameters and conditions for simulation

Boundary condition	Parameters setting
Solver	Pressure-Based
Turbulence Models	k - ε realizable
Multiphase Model	Volume of Fluid
Evaporation/Condensation Model	Lee
Turbulence intensity (%)	5

Thermophysical properties of cooling fluid and tin such as heat transfer coefficient were also reported in Table 3.

Table 3. Thermophysical properties of water and tin

Parameter	Material		Unit
	Water	Tin	
Density	998.2	7033.4	Kg/m3
Heat capacity	4182	210	J/Kg.K
Thermal conductivity coefficient	0.6	66	w/m.k

The effect of nozzle angle, water jet velocity from the nozzle, plate passing velocity, and water temperature on the temperature field in the plate during the quenching process of the under-study tinplate, according to Table 4, was investigated in the current study. After setting up all the parameters and conditions, simulation and solution were performed in 0.3 s with 300 time steps and a time step size of 0.001 with 30 interactions in each time step.

Table 4. Details of the studied parameters and values

Parameter	Unit	Values
Nozzle angle	Degree	15, 30, 45
Water jet velocity	m/s	8, 10
Plate velocity	m/min	244, 200, 160
Water temperature	K	303, 313, 328

3. Results and Discussion

3.1. Mesh Independence Test

Examining mesh independence in CFD analysis is one of the most important parts of any simulation. The average tinplate temperature was used to test mesh independence in the present study. Figure 4 shows the mesh independence study results using five different mesh grids. According to the results, the average temperature difference was significantly decreased by increasing the mesh grid from 236363 to 881479. However, negligible changes in the average temperature were obtained using more mesh grids. Hence, this meshing can provide reliable results and the simulation was performed using the conditions used to produce this meshing. Although simulation with a fine mesh will lead to better results, it creates the need for very advanced computing systems and increases simulation time and cost.

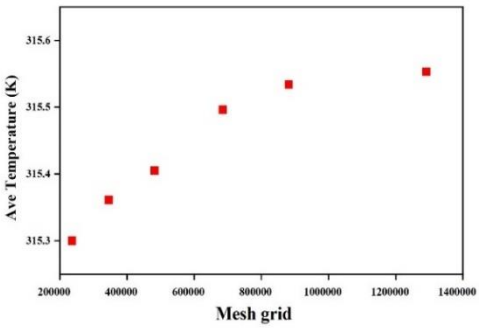

Fig. 4. Results of Convergence test used for simulation

3.2. Validation Study

Validation, as an important field in simulation and numerical studies, examines the accuracy and validity of a simulated process or model for a good representation of the real system [25]. To validate the simulations performed in the current study, the experimental conditions investigated by Álvarez et al [26] were simulated. This study is related to experimental data and numerical analysis of heat transfer for the quenching process of a hot plate in a quench tank containing a water jet impinging on both sides of the plate.

Table 5 reports details related to the plate, the quench tank, and the cooling fluid. In this validation simulation, the middle of the plate temperature is reported at different times.

Table 5. Details related to the plate, the quench tank, and the cooling fluid used for the validation study, based on work by Álvarez et al. [26]

Condition	Unite	Values
Water temperature	K	298
Plate temperature	K	1143
Plate velocity	m/s	0
Number of nozzles	-	9
Nozzle head radius	mm	1.88
Nozzle angle	Degree	90
Water Jet impinging angle	Degree	0
Water jet velocity	m/s	5

Figure 5 shows the results of the simulation in the present study, with the experimental data, as well as the results of the simulation performed by Alvarez et al [26]. Accordingly, a good agreement is observed between the experimental data, the base simulation results, and the simulation results in the current study. Both experimental and simulation results show a continuous decrease in temperature from 1143 K to about 215 K with increasing time during 8 seconds. These outcomes confirm the validity of the simulation conducted in this study.

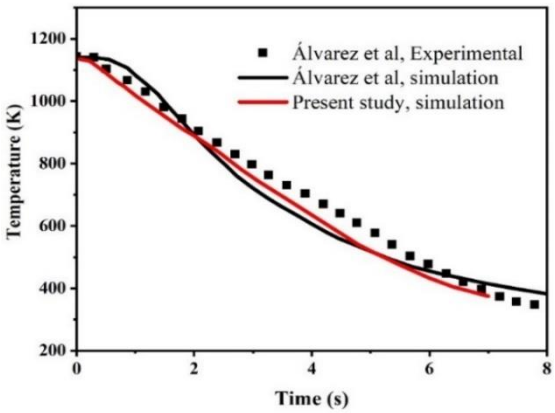

Fig. 5. Comparing the results of the simulation in the present study, with the experimental data, as well as the results of the simulation performed by Alvarez et al. [26]

3.3. Temperature Feld by Time

Figure 6 shows the average temperature of the tinplate for a length of 40 cm during 0.3 s at a water jet velocity of 8 m/s, the tinplate velocity of 244 m/min, a water temperature of 303 K, and a nozzle angle of 45°.

The results show three different cooling rates as a function of time including medium (zone I), fast (zone II), and slow (zone III) cooling rates.

In the first time zone (less than 0.07 s), the medium cooling rate was mainly caused by the initial contact of the hot plate with the cooling water in the quench tank after 0.1 s.

Then, the cooling rate increased dramatically at a time of about 0.07-0.15 s (region II).

It should be noted that in this time zone, the plate is exposed to the water jet impingement. Therefore, cooling occurred at a faster rate. Finally, in the period of about 0.15 to 0.3 (region III), the studied plate passed the water jet zone, and the temperature difference between the plate and water also decreased, so the cooling rate decreased.

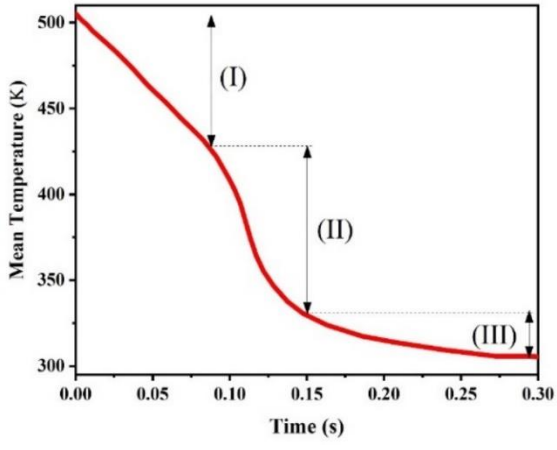

Fig. 6. The average temperature of the tinplate during 0.3 s (Jet velocity: 8 m/s; Tinplate velocity: 244 m/min; Water temperature: 303 K; Nozzles angle: 45°)

Figure 7 shows the field temperature on the tinplate during 0.13 s at a water jet velocity of 8 m/s, the tinplate velocity of 244 m/min, the water temperature of 303 K, and the nozzle angle of 45°.

According to the figure and regarding the plate velocity about 4 m/s, it is clear that the upper part of the plate after 0.11 seconds has not yet been exposed to the water jet and therefore proper cooling and heat transfer were not observed.

These results confirm the positive effect of the water jet on reducing the temperature and increasing the cooling rate of the plate.

However, a more uniform temperature field was observed by time and passing the plate through the water jet.

This was so that after about 0.13 seconds, the average temperature of the plate was approximately reached in the range of 320-330 K.

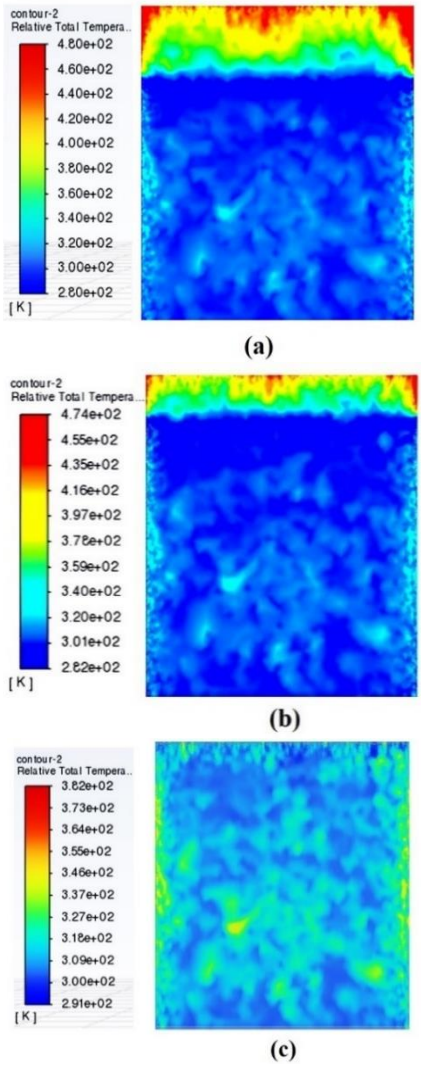

Fig. 7. Field temperature on the tinplate after (a) 0.11 s; (b) 0.12 s; (c) 0.13 s. (Water jet velocity:8 m/s; Tinplate velocity: 244 m/min; Water temperature: 303 K; Nozzles angle: 45°)

3.4. Effect of Nozzle Angle

Figure 8 shows the cooling rate of the template at average temperature during 0.3 s at a water jet velocity of 8 m/s . It also shows a tinplate velocity of 244 m/min, water temperature of 303 K, and different nozzle angles of 15, 30, and 45°. According to the results, a more cooling rate was observed as the nozzle water jet angle increased, in the sequence of 45° > 30° > 15°.

Since the further drop in temperature, the increase in the heat transfer rate in the water jet zone, the removal of bubbles, the removal of defects caused by the bursting of bubbles, and the elimination of quench stains are of great importance, it is better to design the angle of the nozzle so that the water jet hits the plate quickly so that the bubbles are swept from the surface faster. Here, the best cooling rate and more uniform heat transfer were obtained at an angle of 45 degrees, which is due to the earlier arrival of the plate to the water jet impinging zone.

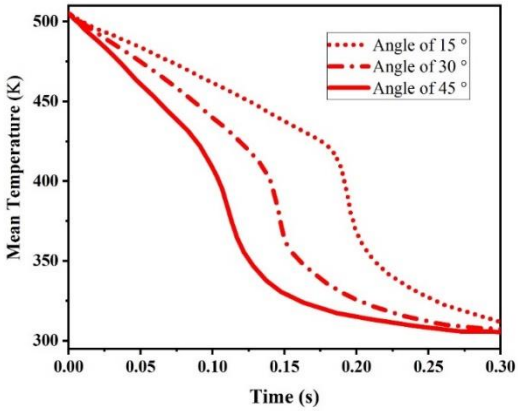

Fig. 8. The cooling rate of the template during 0.3 s at different nozzle angles (Water jet velocity of 8 m/s; Tinplate velocity of 244 m/min; Water temperature of 303 K)

3.5. Effect of Water Jet Velocity

Figure 9 shows the average temperature of the tinplate during 0.3 s at different water jet velocities of 10 and 8 m/s, tinplate velocity of 244 m/min, nozzle angle of 45°, and water temperature of 303 K. As can be seen, with the increase in the water jet velocity, the cooling rate was also increased significantly, so that the time required to decrease the surface temperature from about 505 K to about 305-309 K at a water jet velocity of 10 m/s is considerably lower than 8 m/s. These outcomes indicated a faster cooling rate with increasing water jet velocity.

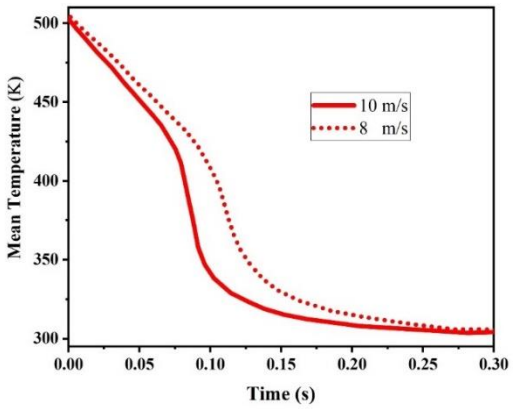

Fig. 9. The cooling rate of the template during 0.3 s at different water jet velocities (Nozzle angles of 45°; Tinplate velocity of 244 m/min; Water temperature of 303 K)

Figure 10 represents the field temperature at the tinplate at different water jet velocities of 10 and 8 m/s. According to the results, it can be seen that increasing the water jet velocity from the nozzle causes a more uniform decrease in the tinplate temperature.

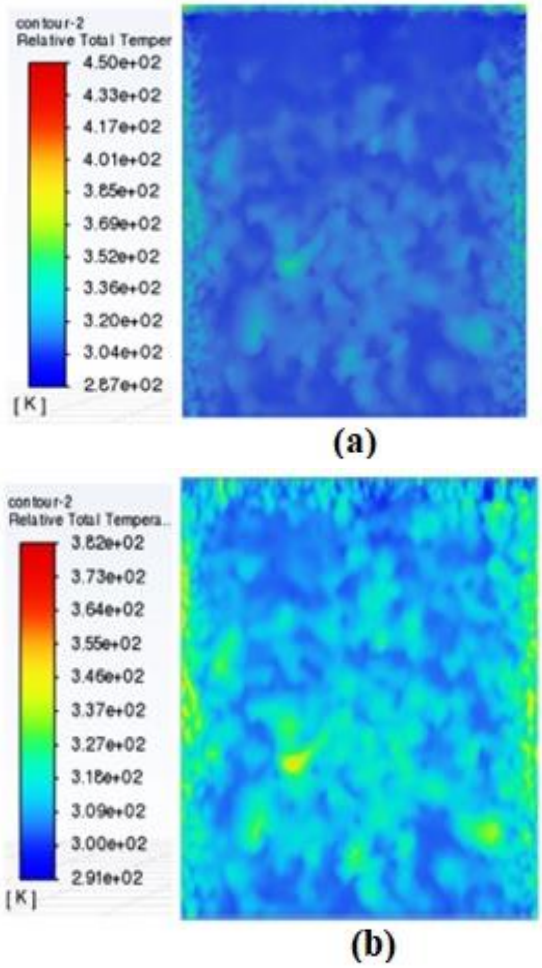

Fig. 10. Field temperature on the tinplate at different water jet velocities of (a) 8 m/s; (b) 10 m/s (Tinplate velocity: 244 m/min; Water temperature: 303 K; Nozzles angle: 45°)

3.6. Effect of Tinplate Velocity

Tinplate velocity is one of the most important influencing variables on heat transfer distribution uniformity in the quenching process. Figure 11 represents the field temperature on the tinplate at different tinplate velocities of 244, 200, and 160 m/min. These results were obtained at water jet velocities of 10 m/s, nozzle angle of 45°, and water temperature of 303 K. As can be seen, reducing the plate velocity from 244 m/min to 200 m/min led to a more uniform temperature distribution, especially at the edges of the tinplate. This better temperature transfer and more uniform distribution can be due to the longer contact time of the plate while passing through the water nozzles. However, it can be seen that the further reduction of the tinplate velocity led to a slight non-uniformity in the temperature distribution.

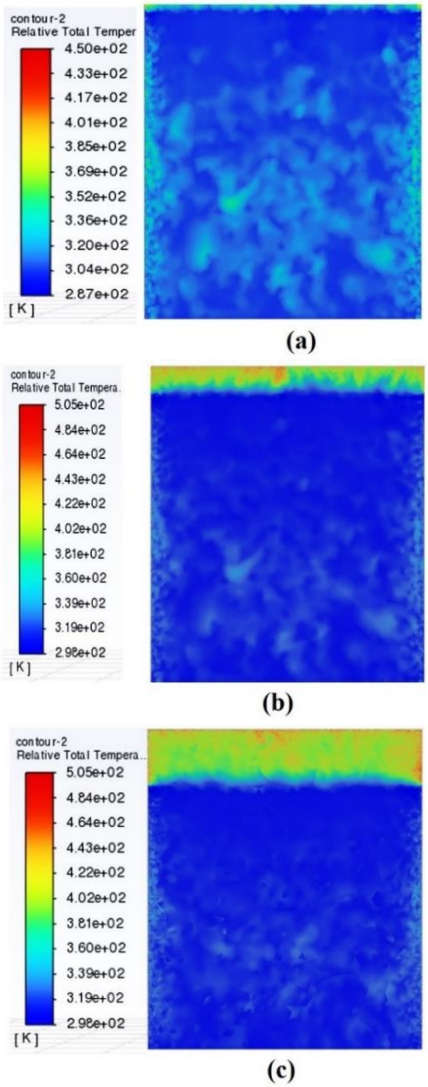

Fig. 11. Field temperature at tinplate velocities of (a) 244 m/min; (b) 200 m/min; (c) 160 m/min. (Water jet velocity: 10 m/s; Water temperature: 303 K; Nozzles angle: 45°)

3.7. Effect of Cooling Fluid Temperature

Since the initial temperature of the tinplate entering the quench tank is equal to (505 K) and the cooling water temperature varies between 303-328 K, the temperature difference is about 177-202 K. Therefore, the bubbles stick to the surface of the plate, which leads to the difficulty of flow, reducing the heat flux and reducing the heat transfer. At the same time, the bubble bursts easily, and this bursting of the bubble exerts an impact force on the molten tin layer, which can lead to the creation of a quench spot and a non-uniform layer on the surface of the plate. Therefore, it is necessary to investigate the effect of water temperature on the tinplate temperature field to reduce stain defects. Figure 12, represents the field temperature on the tinplate at different cooling fluid temperatures of 30, 40, and 55 °C. These results were obtained at water jet velocities of 10 m/s, nozzles angle of 45°, and plate velocity of 200 m/min.

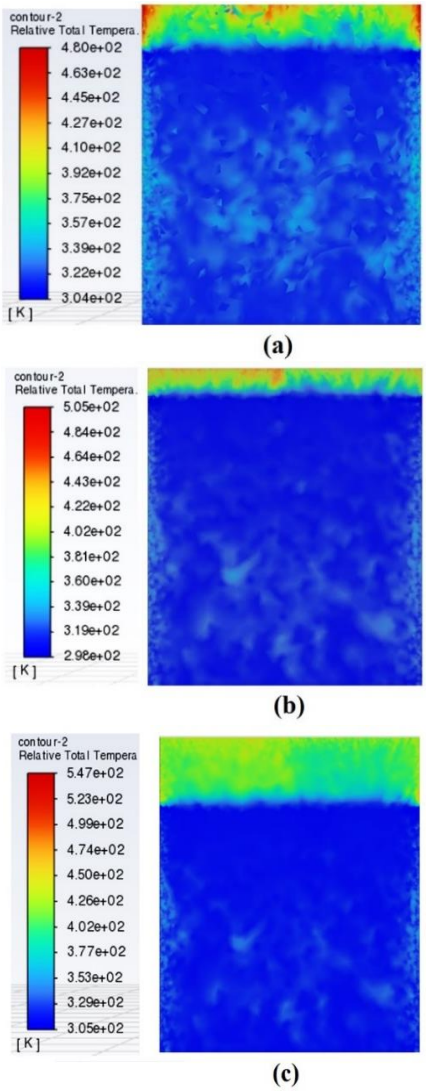

Fig. 12. Field temperature at different temperatures of the cooling fluid. (a) 30 °C,; (b) 40 °C; (c) 55 °C. (Water jet velocity: 10 m/s; Nozzles angle of 45°; Plate velocity of 200 m/min)

According to the results, a more noticeable decrease in temperature is observed in the central areas with an increase in cooling water temperature. However, the temperature field in the areas close to the water-jet zones where the temperature is around 30 °C is lower than the temperatures of 40 and 55 °C.

4. Conclusions

In this research, the quenching process of tinplate was simulated with computational fluid dynamics using the volume of the fluid method with Fluent software, and the effect of nozzle angle (15, 30 and 45°), water jet velocity (8 and 10 m/s), tinplate movement (160, 200, and 244 m/min), and cooling water temperature (30, 40, and 55 °C) in the quench tank on the plate cooling rate and temperature field on the tinplate was evaluated. The simulation conditions are based on the tinplate unit of Mobarakeh Steel Company, Isfahan, Iran. The results confirmed the positive effect of higher water jet velocity on a higher cooling rate and uniform heat transfer, so that the time required to decrease the surface temperature from about 505 K to about 305-309 K at a water jet velocity of 10 m/s is considerably lower than 8 m/s. Furthermore, reducing the tinplate movement velocity from 244 to 200 m/min led to a more uniform temperature distribution in the tinplate. These results indicate that higher tinplate velocity or higher water temperature can reverse cooling rate.

Acknowledgments

The authors would like to thank the generous financial support provided by the University of Kashan for financial support to this study. The authors also wish to express gratitude to the Mobarakeh Steel Company.

Funding Statement

This research did not receive any specific grant from funding agencies in the public, commercial, or not-for-profit sectors.

Conflicts of Interest

The authors declare that they have no potential conflict of interest.

Authors Contribution Statement

Ali Jafari: Data Curation; Investigation; Methodology; Resources; Software; Validation; Visualization; Writing – Original Draft.

Ahmad Reza Rahmati: Conceptualization; Data Curation; Formal Analysis; Investigation; Methodology; Project administration; Resources; Software; Supervision; Validation; Visualization; Writing – Review & Editing.

References

[1] Zhang, W., Bai, Z., Ran, J., Xu, S., Ji, H., Guo, W., Elmi, S. A., 2024. Mechanism of surface rust defects on tinplate strip steel during storage and transportation. *Ironmaking & Steelmaking*, 51(5), PP. 481-492.

[2] Cova Caiazzo, F., Brambilla, L., Montanari, A., Mischler, S., 2018. *Chemical and morphological characterization of commercial tinplate for food packaging. Surface and interface analysis*, 50(4), PP. 430-440.

[3] Li, X., Wang, N., Chen, M., Ma, T., 2021. Tracking large-size inclusions in al deoxidated tinplate steel in industrial practice. *ISIJ International*, 61(7), PP. 2074-2082.

[4] Schoina, L., Jones, R., Burgess, S., Vaughan, D., Andrews, L., Foley, A., Valera Medina, A., 2023. Numerical and techno-economic analysis of batch annealing performance improvements in tinplate manufacturing. *Energies,* 16(20), PP. 7040.

[5] Pandey, S., Mishra, K. K., Ghosh, P., Singh, A. K., Jha, S. K., 2023. Characterization of tin-plated steel. *Frontiers in Materials*, 10, PP. 1113438.

[6] Wu, F., Liu, X., Xiao, X., 2019. Surface coverage characterization of tinplates after post-treatment processes. *Materialwissenschaft und Werkstofftechnik*, 50(9), PP. 1131-1138.

[7] Dey, S., Agrawal, M. K., 2016. Tinplate as a sustainable packaging material: Recent innovation and developments to remain environment friendly and cost effective. *Int. J. Res. IT Manag. Eng*, 8, PP. 9-22.

[8] Zhang, W., Zhang, X., Guo, Z., Wang, J., Bai, Z., 2023. Simulation analysis of temperature field of tinplate in the quenching. *International Journal of Simulation Modelling*, 22(1), PP. 88-99.

[9] Chen, N. L., Zhang, W. M., Li, Q., Gao, C. Y., Liao, B., Pan, J. S., 2006. Optimization of quench tank structure based on CFD simulation. *Solid state phenomena*, 118, PP. 363-368.

[10] Chakraborty, S., Giri, S. S., Bhagat, A., Singh, S., Ghori, J., 2022. Effect of tramp oil ingress in cold rolling oil bath leading to white spot defect on CRCA at Tinplate mill. *Engineering Failure Analysis*, 140, PP. 106601.

[11] Wu, F., Liu, X., Xiao, X., 2018. Surface characterisation of electroplated tinplate with different coating mass. *Surface Engineering*, 34(6), PP. 462-467.

[12] Gomez, C., Van Der Geld, C., Kuerten, J., Bsibsi, M., Van Esch, B., 2020. Quench cooling of fast moving steel plates by water jet impingement. *International Journal of Heat and Mass Transfer*, 163, PP. 120545.

[13] Barrena-Rodríguez, M. d. J., Acosta-González, F. A., Téllez-Rosas, M. M., 2021. A review of the boiling curve with reference to steel quenching. *Metals*, 11(6), PP. 974.

[14] Yang, X.-w., Zhu, J.-c., Dong, H., Lai, Z.-h., Nong, Z.-s., Yong, L., 2013. Optimum design of flow distribution in quenching tank for heat treatment of A357 aluminum alloy large complicated thin-wall workpieces by CFD simulation and ANN approach. *Transactions of Nonferrous Metals Society of China*, 23(5), PP. 1442-1451.

[15] Xiao, B., 2010. Numerical modeling and experimental investigation for optimization in quenching processes of aluminum and steel parts. (Dissertation, Worcester Polytechnic Institute).

[16] Samuel, A., Prabhu, K. N., 2022. Residual stress and distortion during quench hardening of steels: a review. *Journal of Materials Engineering and Performance*, 31(7), PP. 5161-5188.

[17] Rojas-Sola, J. I., García-Baena, C., Hermoso-Orzáez, M. J., 2016. A review of the computational fluid dynamics simulation software: Advantages, disadvantages and main applications. *Journal of Magnetohydrodynamics and Plasma Research*, 21(4), PP. 417-424.

[18] Novosád, J., Peukert, P., Pomp, N., Klouček, P., 2020. CFD simulation of the multiphase heat transfer during the quenching process. In: *IOP Conference Series: Materials Science and Engineering, IOP Publishing, 2020*, pp. 012022.

[19] Kobayashi, K., Nakamura, O., Haraguchi, Y., 2016. Water quenching CFD (computational fluid dynamics) simulation with cylindrical impinging Jets. *Nippon steel & sumitomo metal technical report*, 401, PP. 105-110.

[20] Toghraie, D., 2016. Numerical thermal analysis of water's boiling heat transfer based on a turbulent jet impingement on heated surface. *Physica E: Low-Dimensional Systems and Nanostructures*, 84, PP. 454-465.

[21] Qu Zhe, Z. X., Xing Ruofei, Fu Yudong, 2021. Design and fluid-thermal coupling of a strong quenching tank with double vortex flow field. *Heat Treatment of Metals*, 46(11), PP. 262-269.

[22] Gadala, M., Khan, M.S., slam, F., Gomaa, A., 2022. A Numerical Study of Two-Phase Cooling Phenomena in Steel Quenching Using Water Jet Impingement. Available at SSRN 4153234.

[23] Narumanchi, S., Troshko, A., Bharathan, D., Hassani, V., 2008. Numerical simulations of nucleate boiling in impinging jets: Applications in power electronics cooling. *International Journal of Heat and Mass Transfer*, 51(1-2), PP. 1-12.

[24] Sadrehaghighi, I., 2019. Turbulence Modeling- A Review. *Report*, 1(86), P. 9.

[25] Jan, J., MacKenzie, D. S., 2024. On the Development of Computational Fluid Dynamics Quenching Simulation Methodology for Effective Thermal Residual Stress Control. *Journal of Materials Engineering and Performance*, 33(8), PP. 3986-4010.

[26] Tinajero-Álvarez, R. A., Hernández-Bocanegra, C. A., Ramos-Banderas, J. Á., López-Granados, N. M., Farrera-Buenrostro, B., Torres-Alonso, E., Solorio-Díaz, G., 2024. Numerical Analysis of Convective Heat Transfer in Quenching Treatments of Boron Steel under Different Configurations of Immersed Water Jets and Its Effects on Microstructure. *Fluids*, 9(4), PP. 89.